A VISCOELASTIC MODEL FOR EVALUATING EXTRUSION-BASED PRINT CONDITIONS

Chad Duty[1,2], Christine Ajinjeru[1], Vidya Kishore[1], Brett Compton[1], Nadim Hmeidat[1]
Xun Chen[2], Peng Liu[2], Ahmed Arabi Hassen[2], John Lindahl[2], Vlastimil Kunc[1,2,3]

[1]University of Tennessee
[2]Manufacturing Demonstration Facility, Oak Ridge National Laboratory
[3]Purdue University

Abstract

Extrusion-based printing systems have improved significantly over the past several years, allowing for higher throughput, higher temperatures, and larger components. At the same time, advanced materials are being introduced on the market that can provide improved performance over a range of operating conditions. Often these materials incorporate fiber reinforcements, reactive resins, and additives to control reaction kinetics, flow rheology, or thermal stability. This study presents a general framework for evaluating the printability of various candidate materials based on a basic viscoelastic model. The model addresses fundamental requirements for extrusion-based printing, including pressure-driven flow, bead formation, bead functionality, and component-level functionality. The effectiveness of this model for evaluating the impact of compositional variations and identifying appropriate processing conditions has been demonstrated for specific materials on direct write, fused filament fabrication, and large-scale extrusion platforms.

Background

The Manufacturing Demonstration Facility (MDF) at the Oak Ridge National Laboratory (ORNL) has developed a large-scale additive manufacturing system called Big Area Additive Manufacturing (BAAM) that is capable of depositing thermoplastic materials at a rate of up to 50 kg/h in a build volume that measures 6 m x 2.4 m x 1.8 m. [1, 2] The BAAM system works with pellet-based feedstock materials that can include fiber reinforcements to improve the mechanical and thermal properties of the printed component as well as reduce distortion. [3, 4] The BAAM system is also capable of depositing high temperature materials (up to 500°C) as well as amorphous and semi-crystalline materials. [5-9] As new material development trends toward higher performance composites at elevated temperatures, the cost of feedstock materials can increase by a factor of 5-10x. At the speed and scale of the BAAM system, an Edisonian trial-and-error approach to determine appropriate processing conditions is not feasible. Incomplete print jobs or overly distorted components could result in several hundred pounds of wasted material and days of unproductive print time. More importantly, improper processing conditions that may cause a material to clog or seize within the extrusion system can put the integrity of the system at risk.

Therefore, a comprehensive model is needed to determine whether a candidate material is "printable" on the BAAM system. The model should be based on fundamental material properties that can be measured on small quantities of materials in a controlled setting, allowing for identification of proper processing conditions prior to experimentation on the BAAM system. The goal of this work was to develop a fundamental set of print conditions based on a select number of viscoelastic and thermo-mechanical properties of polymers. The model could then be generalized to address common extrusion-based deposition platforms, such as fused filament fabrication (FFF) and direct write (DW) systems, as well. This paper presents the basic concepts for such a Printability Model. A more detailed description of the model has been submitted for publication [10] and specific example cases of the model have been demonstrated in a related conference paper. [11]

Print Systems & Materials

The general deposition parameters illustrated in Figure 1 are common to all levels of extrusion-based printing platforms, including BAAM, FFF, and DW. Fundamentally, the deposition system is capable of producing a maximum system pressure (P_{max}) to extrude a material at a given volumetric flow rate (Q) through an extrusion orifice that has a given geometry. The nozzle geometry includes not just the exit diameter (D_e) and length (L_e), but also the upstream nozzle diameter (D_n) and length (L_n) as well. The geometry of the part is defined at a local level by the height (h) and width (w) of the deposited bead, and on a global level by the height (H) of the part and the print time for each layer (t_{layer}). The velocity of the deposition head (V_h) is directly related to the volumetric flow rate (Q), the bead geometry (h, w), and the layer time (t_{layer}). These basic parameters can be applied to extrusion-based print platforms regardless of feedstock forms (pellet, filament, resin) or feed mechanism (shear screw, roller, plunger).

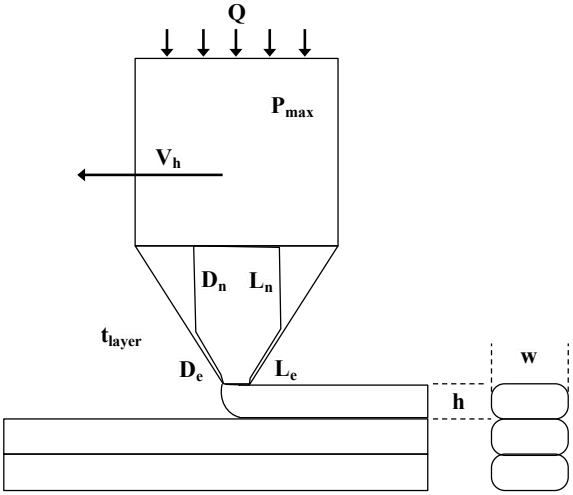

Figure 1. Basic print parameters of extrusion-based systems

The fundamental material properties that are relevant to this Printability Model range from basic physical characteristics, such as density (ρ), to thermo-mechanical properties, such as yield strength (σ_{ys}) and coefficient of thermal expansion (CTE, α). Basic rheological properties at the

processing temperature are also important, including the viscosity (η) as a function of shear rate, the storage modulus (G'), and the loss modulus (G"). The surface energy (γ_{SE}) of the extruded material is also important. These fundamental material properties can be directly measured with a small quantity of material using standard laboratory techniques, such as tensile testing, thermo-mechanical analysis, and parallel plate rheometry. The following sections will outline print criteria that utilize these fundamental properties to determine whether such a material is "printable" under given processing conditions.

Viscoelastic Classification

The extrusion characteristics of a polymer are often time-dependent, so it is important to correctly classify the mechanical response of a material under a given set of processing conditions. The proposed model uses tan δ, which is the ratio of the loss modulus (G") to the storage modulus (G'), to determine the appropriate viscoelastic classification for the material of interest (Figure 2). A tan δ < 0.1 (G' >> G") indicates a very stiff material (elastic solid, E-S) that behaves almost entirely in a recoverable elastic fashion. A tan δ between 0.1 and 1 behaves like a viscoelastic solid (VE-S) according to the Kelvin-Voigt model. A tan δ between 1 and 10 behaves like a viscoelastic liquid (VE-L) according to the Maxwell model. Finally, a tan δ greater than 10 (G' << G") indicates a viscous liquid (V-L). It is important to note that the classification of a given material may change at different points in the extrusion process depending upon the given processing conditions (e.g. temperature, shear rate). For each of the printing conditions listed below, it is important to identify the appropriate classification for the material's viscoelastic response.

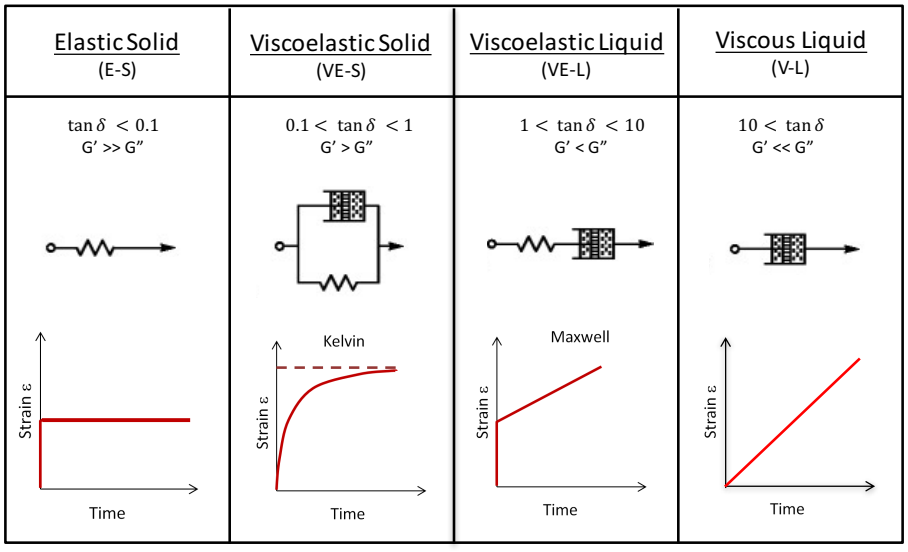

Figure 2. – Viscoelastic classification of materials based on tan δ.

Condition 1 – Material Extrusion

At a basic level for any extrusion process, a primary condition must be that material flows through an orifice under pressure. For advanced extrusion-based print systems, this condition can be subdivided into (1a) viscous flow through a nozzle and (1b) reinforcing fiber clog (Figure 3).

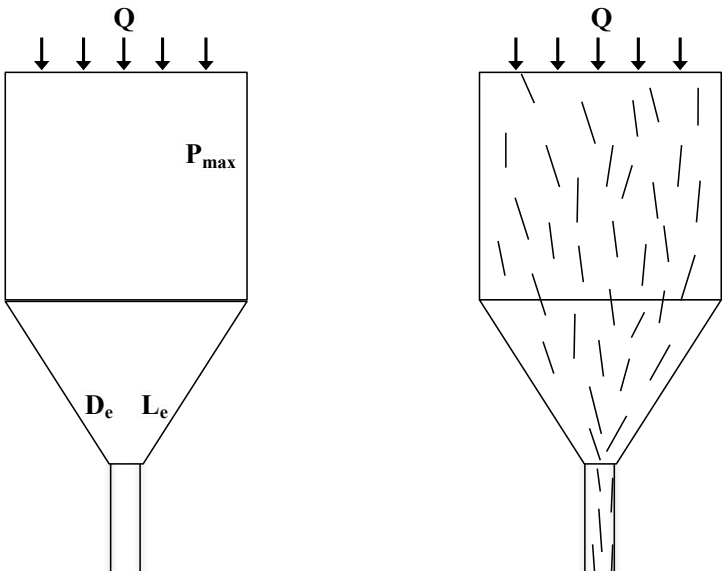

Figure 3. Material extrusion print conditions for viscous flow (left) and fiber clog (right).

(1a) Viscous Flow Through a Nozzle

Pressure-driven flow through a circular orifice can be analyzed using the Hagen-Poiseuille equation [12] that defines the pressure drop (ΔP) required to achieve a given volumetric flow (Q) for a material of a known viscosity (η) through an orifice of given radius (R) and length (L):

$$\Delta p = \frac{8\,\eta\,Q\,L}{\pi\,R^4} \tag{1}$$

Most polymers are shear-thinning as a function of shear rate according to the power law relation: $\eta = C\,\dot{\gamma}^{(n-1)}$, where C is a constant and *n* is the power law index. Therefore, the viscosity in equation (1) is dependent on the calculated shear rate ($\dot{\gamma}$) through a circular orifice, such that:

$$\dot{\gamma} = \frac{4Q}{\pi R^3}\left(\frac{3n+1}{4}\right) \tag{2}$$

Combining the power law relation with equations (1) and (2) allows for the pressure drop of a shear thinning polymer through a circular orifice to be calculated. Therefore, the print criteria for condition (1a) is achieved if the calculated pressure drop is less than the maximum system pressure (P_{max}). Note that failure to meet print condition (1a) does not necessarily mean that the material will not extrude through the orifice, rather that the desired volumetric flow rate (Q) will not be achieved under the specified processing conditions.

(1b) Reinforcing Fiber Clog

The increasing utilization of fiber-reinforced materials for extrusion-based 3D printing makes it necessary to consider the flow characteristics of a fiber rich medium. Aside from the significant viscosity increase that often results from using fiber reinforcements [5, 7, 11], flow of a fiber-filled material through a constricting orifice can result in a fiber network bridging the flow channel, resulting in a clogged nozzle. A first estimate that accounts for the increased pressure that results from flow through a fibrous network is:

$$\langle u \rangle = -\frac{K}{\eta}\left(\frac{d(p)}{dx}\right) \tag{3}$$

where u is flow velocity, K is permeability, η is viscosity, and $d(p)/dx$ is the pressure drop. The average velocity (u) through a circular channel is $Q/\pi R^2$ for a radius R. The length of the exit channel (L_e) can be considered dx. The permeability, K, is equal to: [13]

$$K = \frac{\varepsilon\, d_t^2}{32\, \tau_f} \tag{4}$$

where ε is the porosity, d_t is the diameter of the channel, and τ_f is the tortuosity. As a first-estimate, we can assume the that tortuosity is equal to one and the porosity can be approximated as $(1\text{-}V_f)$, where V_f is the volume fraction of reinforcing fibers in the material. With these simplifications, equations (3) and (4) can be rearranged to find that:

$$\Delta P = \frac{128\, L_e\, Q\, \eta}{\pi\, D_e^4\, (1 - V_f)} = \frac{8\, L_e\, Q\, \eta}{\pi\, R_e^4\, (1 - V_f)} \tag{5}$$

Note that equation (5) is now equivalent to equation (3) divided by the porosity of the fiber reinforcing material $(1\text{-}V_f)$. In a similar fashion to condition (1a), the pressure drop calculated for fiber reinforced flow must be lower than the maximum system pressure to successfully print.

Condition 2 – Bead Geometry

Extrusion-based 3D printing requires more than traditional extrusion of material through an orifice. For 3D printing to be effective, the extruded material must form a stable bead of a consistent height and width, roughly in the form of a rounded rectangle (Figure 4). In addition to forming the initial bead geometry (condition 2a), the deposited bead must be geometrically stable over a given time period (condition 2b).

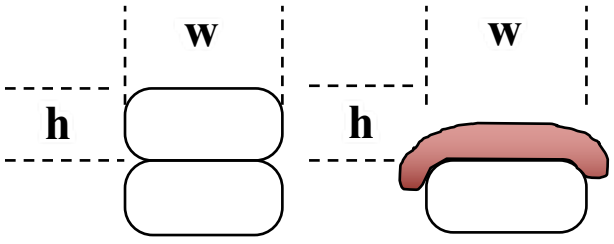

Figure 4. Extruded material must form a geometry (left) that is stable over time (right).

(2a) Geometry Creation

When material is successfully extruded from a 3D printing nozzle, it transitions from a highly constrained environment within the nozzle to a relatively self-supporting free state as the upper layer of a printed structure. The thickness of a deposited layer is typically defined by the physical space between the nozzle and the previously deposited layer. Generally, the polymer is viscous enough to be compressed to the desired layer height as the deposition head passes over the extruded material (discussed more below in condition 3b). If the material is too stiff to permit this moderate compression, it likely would not have passed condition 1, so the present criteria focuses on satisfying the lower limit – where the material may flow too freely from the extrusion head and not achieve the desired layer height.

One estimate of this print condition is to calculate the free-standing height (h_{fs}) of a material based on the material's density (ρ) and surface energy (γ_{SE}), according to:

$$h_{fs} = 2\sqrt{\frac{\gamma_{SE}}{g\,\rho}} \tag{6}$$

If the free-standing height (h_{fs}) is less than the desired layer height (h), then the material will not be able to form a consistent bead geometry and fails this print condition.

(2b) Geometry Stability

The initial formation of a consistent bead geometry is often achieved, but the geometry is not stable enough to maintain dimensional tolerances over time. In the case of thermoplastic materials, the mechanical properties dramatically improve over a short time period as the temperature of the deposited material cools from the deposition temperature (T_{dep}) to below the glass transition temperature (T_g). For the purpose of this model, it is assumed that the time between successively deposited layers (t_{layer}) is a conservative estimate for this cooling time, and the material properties of the extruded material are conservatively taken at the deposition temperature (T_{dep}) during this time period. For thermoset materials, the chemical kinetics of the cure or crosslinking reaction will define the appropriate time period for bead stability.

As a conservative estimate for geometry stability, it is assumed that the extruded bead must support the weight of the entire bead over the time period of interest (t_{layer}). The hydrostatic pressure (σ_{HP}) that the bead must support can be simply calculated by: $\sigma_{HP} = \rho_{melt} * g * h$, where ρ_{melt} is the density at T_{dep}, g is gravity, and h is the layer height. The acceptable strain limit (ε_{limit}) is a relatively arbitrary value that can be defined by the user, but is generally in the range of 10% for successful printing. The actual strain of the material subjected to σ_{HP} over time depends on the viscoelastic classification of the material as outlined above as a function of tan δ.

For elastic solid materials (E-S), the elastic strain is simply equal to $\varepsilon_{E\text{-}S} = (\sigma_{HP}/G_0')$, where G_0' is the storage modulus at low shear rate. If $\varepsilon_{E\text{-}S} < \varepsilon_{limit}$, the material satisfies print condition 2b.

For viscoelastic solids (VE-S), the elastic strain ($\varepsilon_{E\text{-}S}$) serves as an upper limit that is approached over a period of time (t_{layer}). Therefore, if $\varepsilon_{E\text{-}S} < \varepsilon_{limit}$, the VE-S material satisfies

condition 2b without further concern. However, in the case that $\varepsilon_{E\text{-}S} > \varepsilon_{limit}$, the processing time becomes important. According to the Kelvin-Voigt model, the strain as a function of time can be expressed as:

$$\varepsilon_{VE-S}(t) = \frac{\sigma}{G'_0}(1 - e^{-\frac{t_p}{\tau}}) \tag{7}$$

where t_p is the processing time (equal to t_{layer} here) and τ is the relaxation time. As a first approximation, the relaxation time (τ_0) is equal to η_0 / G_0', where η_0 is the viscosity at low shear rate. Rearranging equation (7) in terms of a print criteria for a strain limit (ε_{limit}) results in:

$$\tau_0 > \frac{-t_{layer}}{\ln\left(1 - \frac{\varepsilon_{limit} G_0'}{\sigma_{HP}}\right)} \tag{8}$$

For viscoelastic liquids (VE-L), the elastic portion of the strain is assumed to occur instantaneously while the viscous strain continues to evolve over time. Therefore, if the elastic strain $\varepsilon_{E\text{-}S} > \varepsilon_{limit}$, the VE-L immediately fails this print condition. However, satisfying the condition $\varepsilon_{E\text{-}S} < \varepsilon_{limit}$, is not sufficient for VE-L materials since the strain continues to evolve according to:

$$\varepsilon_{VE-L}(t) = \frac{\sigma}{G'_0} + \frac{\sigma}{\eta_0} t_p \tag{9}$$

Once again, if the processing time is taken as the time between layers (t_{layer}), equation (9) can be re-written as a print criteria for VE-L materials in terms of the low shear rate viscosity (η_0):

$$\eta_0 > \frac{\sigma_{HP} t_{layer}}{\left(\varepsilon_{limit} - \frac{\sigma_{HP}}{G_0'}\right)} \tag{10}$$

Finally, for viscous liquids (V-L), the elastic portion is irrelevant and only the time dependent strain must be considered. In this case, equation (10) can be simplified to be:

$$\eta_0 > \frac{\sigma_{HP} t_{layer}}{(\varepsilon_{limit})} \tag{11}$$

Condition 3 – Bead Functionality

There are a number of functions that an extruded bead must perform in order to make 3D printing possible. The majority of 3D printed materials employ some variation of sparse in-fill patterns that require the extruded material to bridge an unsupported gap (condition 3a). Additionally, the deposited bead on a given layer serves as a substrate for deposits on successive layers (condition 3b). Finally, as multiple layers are deposited, the extruded bead must provide a strong foundation for the layers above it (condition 3c).

(3a) Bridging a Gap

Sparse in-fill patterns in 3D printed parts often require that an extruded bead is able to span an unsupported gap. Generally speaking, the span between supports (L_{span}) and the allowable deflection at the center of the span (δ_{limit}) can be represented as a multiple of bead height (h). In this model, L_{span} is defined as (10*h) and δ_{limit} is (h/4). For elastic materials, the unsupported bead can be considered an elastic beam that is supported at the ends by simple pin joints (Figure 5). Using the elastic beam theory [14], the deflection at the center of the beam is:

$$\delta_{center} = C\frac{\left(F_L * L_{span}\right) * {L_{span}}^3}{G_0' * I} \tag{12}$$

where F_L is the distributed load, C is a constraint-based constant (equal to 5/384 for a pinned beam) [14] and I is the second moment of area. For a self-supporting beam, the distributed load across the beam is $F_L = \rho_{melt} * g * h * w$, and I is equal to 1/12 * w * h^3 for a rectangular beam.

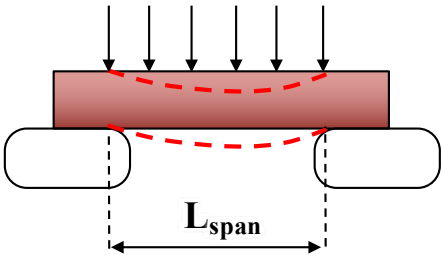

Figure 5. Deflection of a deposited bead spanning a gap.

The elastic beam theory is clearly inappropriate for viscous materials (where tan δ > 1), so a simple model is suggested that is analogous to characterizing the sag in a long-spanning cable. The tension that develops in a self-supporting cable over a distance (L_{span}) is equal to:

$$T_{cable} = \frac{F_L * {L_{span}}^2}{8 * \delta_{limit}} \tag{13}$$

when the center deflection is at the allowable limit (δ_{limit}). Since the tension in the cable reduces as the cable sag increases, it can conservatively be estimated that the average tension in the cable is twice the tension at full deflection. Using the constitutive equations for strain in viscous materials, the time required to achieve a center deflection under this load (t_{sag}) would need to be less than the layer time (t_{layer}):

$$t_{layer} > t_{sag} = \frac{\delta_{limit} * \eta * w}{2 * T_{cable}} \tag{14}$$

(3b) Substrate Support

In addition to supporting its own weight, an extruded bead needs to have enough mechanical strength to provide a stable foundation for extruded materials on the following layer (Figure 6). All extrusion-based 3D printing systems orient the extrusion nozzle perpendicular to the deposited layer, meaning that the extruded material must re-orient by 90 degrees – requiring a change in momentum (σ_{mo}) of ½ ρ V_E^2, where V_E is the velocity through the exit of the nozzle. The circular extruded material bead must also be compressed to a semi-rectangular shape having a thickness

equal to the desired layer thickness. An analogue is proposed for this compression action that is similar to bi-directional rectilinear flow in compression molding of polymers. [15] The analogous compression force for compression molding is:

$$F_{comp} = 4\,\eta\,V_{comp}\,\frac{U}{h^2} \tag{15}$$

where η is the viscosity at the extrusion shear rate ($\dot{\gamma}$), V_{comp} is the volume being compressed, U is the clamping speed, h is the gap between plates, and the friction between the mold plates has been ignored. Since the clamping speed (U) is so fast ($t_{comp} = D_e / V_h$), only the elastic response is considered relevant for this analysis. The volume of the material being compressed (V_{comp}) can be represented as:

$$V_{comp} = \frac{\pi}{4}\,\frac{Q * D_e}{V_h} \tag{16}$$

and the overall compression stress (σ_{comp}) can then be calculated as:

$$\sigma_{comp} = \frac{\pi}{h^2}\,\frac{\eta\,Q}{w\,D_e}\left(\frac{Q}{V_h\,D_e} - h\right) \tag{17}$$

The total stress that the substrate must withstand for 3D printing (σ_{sub}) is a combination of σ_{comp} and σ_{mo}, which must be less than the yield stress of the extruded material (σ_{YS}).

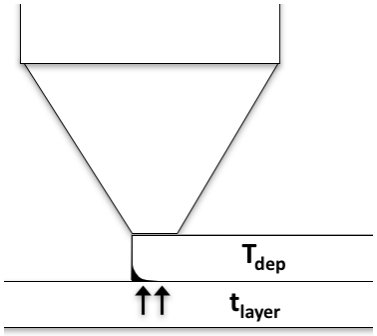

Figure 6. Deposited bead needs to resist the extrusion force of the following layer.

(3c) Wall Support

Not only must an extruded bead support the extrusion forces of the successive layer, but it must also support the combined weight of multiple layers above it without deforming more than an acceptable amount (Figure 7). In the simplest sense, the stress applied to the lower layers is a multiplier of the hydrostatic pressure calculated under condition 2b ($\sigma_{wall} = n_{layers} * \rho * g * h$), where n_{layers} is the number of layers being supported. Since most thermoplastic materials have cooled to T_g by the time they are supporting a sizeable wall, it can be assumed that (tan δ) is well below 1 and only elastic properties are relevant. Therefore, the two print criteria for this print condition are based on strain ($\varepsilon_{limit} < \sigma_{wall}/G_0'$) and strength | ($\sigma_{YS} > \sigma_{wall}$).

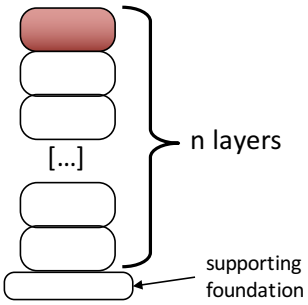

Figure 7. Deposited beads must support combined weight of successive deposits.

Condition 4 – Component Functionality

A 3D printed structure must be able to maintain some degree of dimensional stability and integrity to successfully print. It is well known that as the size of the printed structure increases, the distortion due to thermal contraction becomes exaggerated and causes parts to warp, curl, and crack (Figure 8).

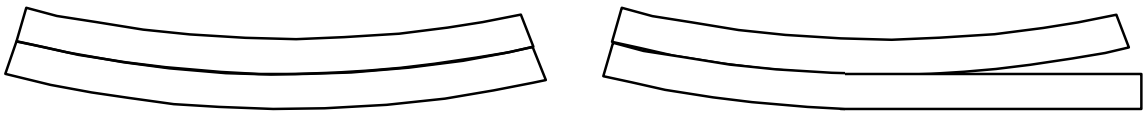

Figure 8. Strain following deposition can cause the structure to distort (left) and crack (right).

(4a) Distortion

Extrusion-based printing of thermoplastic materials often involves depositing molten material on top of previously deposited material that has cooled below the glass transition temperature (T_g). As the size and layer time of deposition systems increase (such as with BAAM), the previously deposited structure can cool close to the ambient room temperature. As a first approximation, this model assumes that deposited material between the deposition temperature and T_g forms a bond with underlying material, but does not have sufficient mechanical strength to accumulate significant stress that would result in distortion. Therefore, the thermal contraction responsible for distortion of the structure is a function of the coefficient of thermal expansion (CTE) of the material and the temperature change (T_g-T_{amb}). Wang [16] proposed a simple model for the deformation of a successively deposited structure:

$$\delta = \frac{n^3 h}{6\alpha(T_g - T_{amb})(n-1)}\left(1 - cos\frac{3\alpha L}{n}(T_g - T_{amb})\frac{n-1}{n^2}\right) \tag{18}$$

where L is the length of the structure, n is the number of layers and α is the CTE. Since the deflection in equation (18) is maximum when (n=2), the maximum deflection divided by the layer height can be defined as D_{max}, such that:

$$\Delta_{max} = \left(\frac{\delta}{h}\right)_{n=2} = \frac{4}{3A}\left(1 - \cos\left(\frac{3}{8}A\lambda\right)\right) \tag{19}$$

where $A = \alpha (T_g - T_{amb})$ and λ is (L/h). This allows a print criteria for distortion to be defined such that Δ_{max} must be less than 1. If the distortion (δ) exceeds the layer height, the print head will likely collide with the previously deposited material.

(4b) Cracking

As printed structures experience dimensional changes due to either thermal or chemical events (cooling or curing), significant residual stress can accumulate in the structure. If the stress between successive layers exceeds the bond strength between layers, a crack will initiate – likely near a discontinuity in the print and grow along the interface. General criteria have not yet been developed for quantifying the residual stress that may result in a crack, but it is anticipated that it will involve either a comparison between local stress at the interface, or comparing the available energy release rate to the critical energy at the interface.

Conclusion

A general framework has been presented for evaluating the "printability" of materials using extrusion-based deposition systems. Four primary categories (Figure 9) are proposed which address (1) extrusion of material through a nozzle, (2) formation and stability of the extruded bead, (3) the functionality of the deposited bead, and (4) the distortion and cracking of the printed structure. Simple evaluation criteria have been proposed for each of the print conditions which have proven effective at identifying appropriate print conditions for various materials across all three deposition platforms (see [10, 11] for further details). The criteria utilized in this model are a first approximation and will likely be refined over the coming years to provide meaningful guidance toward future material and system development.

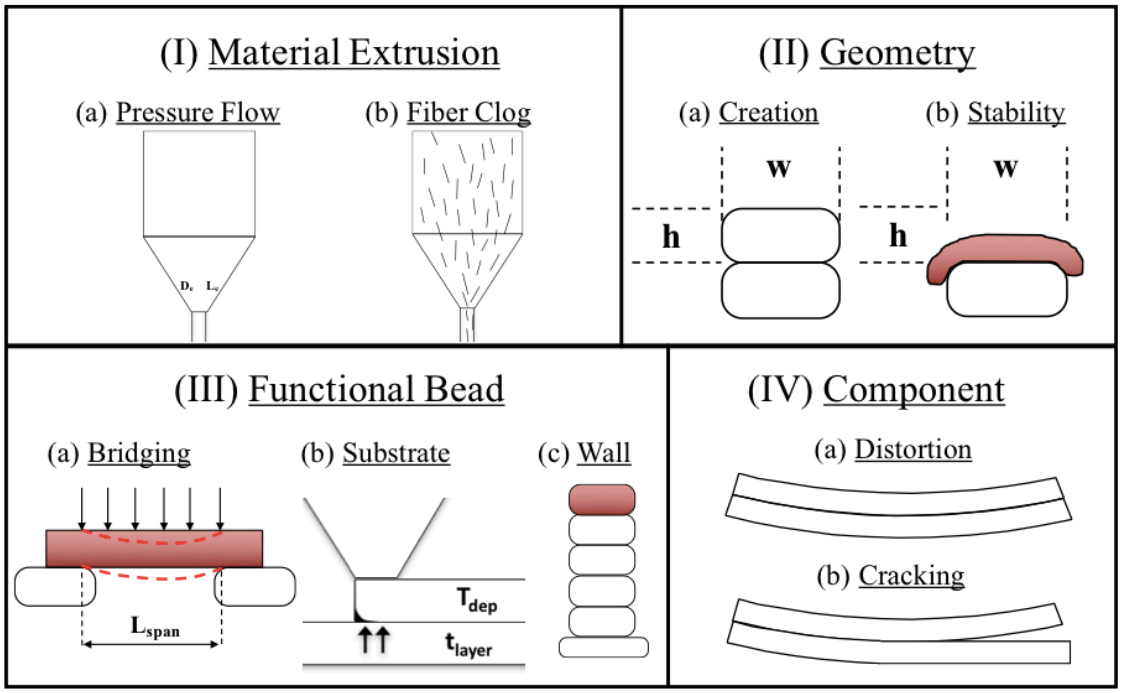

Figure 9. Classifications for extrusion-based print criteria.

Acknowledgements

A portion of the research was sponsored by the U.S. Department of Energy, Office of Energy Efficiency and Renewable Energy, Advanced Manufacturing Office, under contract DE-AC05-00OR22725 with UT-Battelle, LLC.

References

1. Newell, C., et al., *Out of bounds additive manufacturing.* Advanced Materials & Processes, 2013: p. 15.
2. Love, L.J., et al. *Breaking Barriers in Polymer Additive Manufacturing*. in *SAMPE*. 2015. Baltimore, MD.
3. Love, L.J., et al., *The importance of carbon fiber to polymer additive manufacturing.* Journal of Materials Research, 2014. **29**(17): p. 1893-1898.
4. Duty, C.E., et al., *Structure and mechanical behavior of Big Area Additive Manufacturing (BAAM) materials.* Rapid Prototyping Journal, 2017. **23**(1).
5. Kishore, V., et al. *Additive Manufacturing of High Performance Semicrystalline Thermoplastics and Their Composites*. in *Solid Freeform Fabrication Symposium*. 2016. Austin, TX.
6. Kishore, V., et al. *Rheological Characteristics of Fiber Reinforced Poly(ether ketone ketone) (PEKK) for Melt Extrusion Additive Manufacturing*. in *SAMPE*. 2017. Seattle, WA.
7. Ajinjeru, C., et al. *The Influence of Rheology on Melt Processing Conditions of Carbon Fiber Reinforced Polyetherimide for Big Area Additive Manufacturing (BAAM)*. in *SAMPE*. 2017. Seattle, WA.
8. Ajinjeru, C., et al. *The Influence of Rheology on Melt Processing Conditions of Amorphous Thermoplastics for Big Area Additive Manufacturing (BAAM).* in *Solid Freeform Fabrication Symposium*. 2016. Austin, TX.
9. Ahmed Arabi Hassen, et al., *Additive Manufacturing of Composite Tooling Using High Temperature Thermoplastic Materials*, in *SAMPE Conference*. May 2016: Long Beach, CA,.
10. Duty, C., et al., *What Makes a Material Printable? A Viscoelastic Model for Extrusion-Based 3D Printing of Polymers*. 2017: Journal of Manufacturing Processes.
11. Ajinjeru, C., et al. *Rheological Evaluation of High Temperature Polymers to Identify Successful Extrusion Parameters*. in *Solid Freeform Fabrication Symposium*. 2017. Austin, TX.
12. Dealy, J. and K. Wissbrun, *Melt Rheology and Its Role in Plastic Processing*. 1990, New York, NY: Springer Science + Business Media.
13. Ozgumus, T., M. Mobedi, and U. Ozkol, *Determination of Kozney Constant Based on Porosity and Pore to Throat Size Ration in Porous Medium with Rectangular Rods.* Engineering Applications of Computational Fluid Mechanics, 2014. **8**(2): p. 308-318.
14. Beer, F. and E. Johnson, *Mechanics of Materials*. 5th ed. 1992, New York, NY: McGraw Hill Inc.
15. Castro, J. and G. Tomlinson, *Predicting Molding Forces in SMC Compression Molding.* Polymer Engineering & Science, 1990. **30**(24): p. 1568-1573.
16. Wang, T.-M., J.-T. Xi, and Y. Jin, *A Model Research for Prototype Warp Deformation in the FDM Process.* International Journal of Advanced Manufacturing Technology, 2007. **33**: p. 1087-1096.